Revealing the dynamics of gene expression during embryonic genome activation and first differentiation in the rabbit embryo with a dedicated array screening

Roger Léandri, Catherine Archilla, Linh Chi Bui, Nathalie N. Peynot, Zichuan Liu, Cédric Cabau, Annie Chastellier, Jean Paul J. P. Renard, Véronique Duranthon

▶ To cite this version:

Revealing the dynamics of gene expression during embryonic genome activation and first differentiation in the rabbit embryo with a dedicated array screening

R. D. Léandri,[1] C. Archilla,[1] L. C. Bui,[1] N. Peynot,[1] Z. Liu,[1] C. Cabau,[2] A. Chastellier,[3] J. P. Renard,[1] and V. Duranthon[1]

[1]*INRA UMR 1198, Biologie du Développement et Reproduction,* [2]*Agenae, Unité Mathématique, Informatique et Génome, and* [3]*UMR INRA/CEA Radiobiologie et Etude du Génome/Centre de Ressources Biologiques pour la Génomique des Animaux d'Elevages et d'Intérêt Economique, Jouy-en-Josas, France*

Léandri RD, Archilla C, Bui LC, Peynot N, Liu Z, Cabau C, Chastellier A, Renard JP, Duranthon V. Revealing the dynamics of gene expression during embryonic genome activation and first differentiation in the rabbit embryo with a dedicated array screening. *Physiol Genomics* 36: 98–113, 2009. First published November 11, 2008; doi:10.1152/physiolgenomics.90310.2008.—Early mammalian development is characterized by extensive changes in nuclear functions that result from epigenetic modifications of the newly formed embryonic genome. While the first embryonic cells are totipotent, this status spans only a few cell cycles. At the blastocyst stage, the embryo already contains differentiated trophectoderm cells and pluripotent inner cell mass cells. Concomitantly, the embryonic genome becomes progressively transcriptionally active. During this unique period of development, the gene expression pattern has been mainly characterized in the mouse, in which embryonic genome activation (EGA) spans a single cell cycle after abrupt epigenetic modifications. To further characterize this period, we chose to analyze it in the rabbit, in which, as in most mammals, EGA is more progressive and occurs closer to the first cell differentiation events. In this species, for which no transcriptomic arrays were available, we focused on genes expressed at EGA and first differentiation and established a 2,000-gene dedicated cDNA array. Screening this with pre-EGA, early post-EGA, and blastocyst embryos divided genes into seven clusters of expression according to their regulation during this period and revealed their dynamics of expression during EGA and first differentiation. Our results point to transient properties of embryo transcriptome at EGA, due not only to the transition between maternal and embryonic transcripts but also to the transient expression of a subset of embryonic genes whose functions remained largely uncharacterized. They also provide a first view of the functional consequences of the changes in gene expression program.

blastocyst; morula; transient expression; maternal embryo transition

EARLY MAMMALIAN DEVELOPMENT is characterized by extensive modifications in nuclear functions. In the few hours after fertilization, highly differentiated gamete nuclei are transformed into a totipotent zygote nucleus able to give rise to a whole organism. This transient totipotent state is equally shared by the early blastomeres (19, 36) and spans a few cell cycles. However, it disappears at the blastocyst stage, when the early embryo displays two distinct cell types: the trophectoderm cells that are the first differentiated cells of the organism and the pluripotent inner cell mass cells (27). This rapid transition in embryonic nuclear function resulting from epigenetic modifications is concomitant to a transition in genetic control of embryo development. Since the newly formed embryonic nucleus is first transcriptionally silent (22), the earliest developmental events are triggered by a maternally encoded gene expression program regulated at the posttranscriptional level. During the first cleavages, the embryonic nuclei become progressively transcriptionally active, so that embryonic development progressively becomes controlled by the embryonic genome (see Ref. 21 for review).

During this very unique period of development the embryo transcriptome has been mainly characterized in the mouse embryo (17, 34, 37, 38). From these analyses, it appears that gene expression is finely regulated as soon as the embryonic genome is transcribed, and results in a specific transcriptome (13, 14, 20).

The mouse embryo, however, is a particular model. The transcriptional activation of its genome spans a single cell cycle, so that development beyond the two-cell stage already depends on the embryonic genome (3, 15). This abrupt transcriptional activation thus takes place long before the appearance of the first differentiated cells at the blastocyst stage. In addition, it occurs concomitantly with extensive and asymmetric modifications of parental genome epigenetic status. This is first evidenced by an active demethylation of the paternal genome during the one-cell stage as well as an extensive and more progressive demethylation of the maternal genome over the first cell divisions (30). In contrast, in most mammalian species, including humans (4), embryonic genome transcriptional activation spans several cell cycles (5, 7–9, 24). In species with delayed genome transcriptional activation, the embryo relies on maternally inherited factors for a longer period than in the mouse and the activation of the embryonic genome occurs closer to the first cell differentiation events. Moreover, many recent epigenetic studies have underlined the specificity of the mouse, because most mammals show progressive epigenetic modifications over several embryonic cell cycles, to an extent that varies with species (16).

To characterize the transcriptome of early embryonic cells, during their genome activation as well as the progressive restriction of their totipotency, it is necessary to provide further data on species with delayed transcriptional activation and with

---

various extents of embryonic genome epigenetic modifications. We therefore chose the rabbit as an alternative model to analyze variations in gene expression during the period of embryonic genome activation (EGA) and appearance of the first differentiations. In this species, the transcriptional activation of the embryonic genome only is required to lead further embryo development from the 8- to 16-cell stage onward (24), although the embryonic genome is already able to transcribe at the end of the 1-cell stage (8). Furthermore, epigenetic alterations that accompany this transition period are quite different from those observed in the mouse embryo: the paternal genome either remains highly methylated (1, 30) or may be transiently demethylated and then remethylated (29) during the one-cell stage, and the global demethylation of the embryonic genome over the period of cleavage and EGA is very limited (1, 31).

The rabbit has been retained for deep-coverage sequencing of its genome mainly because of its interest in biomedical research, including analysis of drug effects on embryo and fetal development (http://www.genome.gov/25521745). Transcriptomic tools are, however, still not commercially available in this species, for which genome annotation is in progress. To characterize transcriptome variations during EGA and first differentiations in in vivo-developed rabbit embryos, we thus established a rabbit cDNA array dedicated to this critical period of development and screened it with pre- and early post-EGA embryos as well as blastocysts. Our results point to transient properties of the transcriptome at EGA, and provide first information concerning the functional relay between maternal and embryonic information over this period in the rabbit species.

MATERIALS AND METHODS

Embryo collection. The experiment was performed in accordance with the International Guiding Principles for Biomedical Research involving animals as promulgated by the Society for the Study of Reproduction and with the European Convention on Animal Experimentation. Researchers involved in direct work with the animals possessed an animal experimentation license from the French veterinary services.

New Zealand White female rabbit (INRA line 1077) were superovulated as described by Henrion et al. (18) and mated with normal males. In vivo four-cell stage, early morulae (20–30 cells), late morulae, and blastocyst stage embryos were recovered from oviducts and uterus flushed with PBS at 32, 50, 65 and 90 hours postcoitum (hpc), respectively. In vitro embryos were recovered at the one-cell stage (19 hpc) from superovulated females. They were cultured from the one-cell stage onward (19 hpc) until the early morula (58 hpc) and blastocyst (100 hpc) stages in four different culture media: B2 medium (Laboratoire C.C.D., Paris, France), B2 medium plus 2.5% fetal calf serum; ISM$_1$/ISM$_2$ sequential medium (Medicult, Jyllinge, Denmark) with a transition from ISM$_1$ to ISM$_2$ at the eight-cell stage; and G$_1$/G$_2$ sequential medium (Vitrolife, Kungsbacka, Sweden) with a transition at the early morula stage (the sequences used for embryo culture mimicked those used in human in vitro fertilization in terms of genome transcriptional activation timing).

Construction of libraries and clone sequencing. Total RNA was extracted from batches of embryos ($n = 60$–140 depending on embryo stage and culture condition) with the RNeasy Mini Kit (Qiagen) and a DNase I treatment (37°C, 30 min).

Two different cDNA subtracted libraries were constructed. Tester materials (early morulae and blastocysts) contained equal proportions of total RNA from embryos produced in each of the in vivo or in vitro conditions: 110 ng from each condition for the EGA library and 145

ng for the first differentiation (FD) library. In vitro-produced embryos were included in the tester materials because we aimed at using our dedicated array also for the analysis of in vitro-developed embryos (Leandri et al., manuscript in preparation). Driver materials (4-cell embryos and late morulae) exclusively contained total RNA from in vivo-developed embryos: 550 ng for the EGA library and 725 ng for the FD library.

Starting from total RNA, cDNA synthesis and amplification was carried out with the SMART PCR cDNA amplification procedure (SMART-PCR cDNA Synthesis Kit, Clontech, Palo Alto, CA). Subtracted libraries were constructed by suppressive subtractive hybridization (SSH) with the PCR Select cDNA Subtraction Kit (Clontech) as described by Bui et al. (6). PCR-amplified subtracted products were cloned into the pGEM-T-Easy vector (Promega France, Charbonnières, France). DH5α Max-Efficiency *Escherichia coli* bacteria (Invitrogen, Cergy Pontoise, France) were transformed. After overnight culture, they were arrayed in 384-well plates. Replicates of these arrayed libraries were spotted onto nylon membranes (Hybond N+, Amersham, Little Chalfont, UK). Since no endogenous transcript with constant expression during preimplantation development is known in the rabbit embryo, the addition of exogenous reporter transcripts mimicking tester-driver common transcripts or tester-specific transcripts allowed us to validate the quality of the subtraction procedure in both of the libraries (6). We showed that the SSH procedure makes it possible to clone very scarce tester-specific transcripts (0.0005% of the total mRNAs). However, some subtraction failures occurred for very abundant transcripts (6). Therefore, we used a two-step sequencing procedure to reduce the redundancy among the sequenced clones. First, 1,920 clones from the FD library were sequenced. Sequences were analyzed with the SURF software suite (see http://www.sigenae.org/fileadmin/Sigenae/Documentation/SURF_Users_Guide-0.6.pdf for details), resulting in 1,550 "good quality" expressed sequence tags (ESTs). The corresponding 1,550 bacterial clones were then pooled and cultured in liquid Luria Bertani medium before plasmid extraction (Wizard Plasmid Miniprep, Promega). cDNA inserts were PCR amplified with NP1 and NP2R primers (PCR Select cDNA Subtraction Kit, Clontech). This amplified material was [α-^{33}P]ATP labeled (Atlas SMART Probe Amplification Kit, Clontech). This radiolabeled target was hybridized to 4,608 new FD library clones and 4,608 EGA library clones spotted on nylon macroarrays. Nine hundred sixty clones from the FD library and 2,400 clones from the EGA library were selected as negative and sequenced. Eight hundred fifty-six and 2,029 good-quality sequences were selected by the SURF procedure. The resulting 2,406 FD ESTs and 2,029 EGA ESTs were then assembled into contigs with the publicly available rabbit ESTs, using Megablast and CAP-3 tools (see http://www.sigenae.org/fileadmin/Sigenae/Documentation/SIGENAE_ContigBrowser_User_Manual_0.4.pdf for details). Two thousand twenty-two contigs containing at least one of these ESTs were built.

For each of the 2,022 contigs, the longest EST was selected. The corresponding clones were cultured in a fresh 2YT medium containing ampicillin. They were submitted to an hyposmotic freezing/thawing lysis. cDNA inserts were amplified by PCR using universal M13 and M13 reverse primers and PCR Master Mix (Promega) starting from 10 µl of bacterial lysis. Quality of the PCR inserts was checked on a 2% agarose gel. PCR products were concentrated with a speed-vac concentrator and spotted on a nylon microarray with a Microgrid II robot (Biorobotics, Cambridge, UK) to obtain a 2,304-spot probe (containing negative and positive controls).

Unigene annotations of the rabbit embryo cDNA contigs. Contig sequences obtained from the EST clustering were blasted on the Human Unigene Database and the Mouse Unigene Database. Since the length of the rabbit contig sequences varies widely, we did not retain informative annotations according to the length-dependent score but according to the E value, which is length independent. Only annotations with a blast E value inferior to 10^{-30} were retained as informative.

Target amplifications. Targets were composed of batches of in vivo embryos (16 blastocysts, 34 early morulae, or 52 four-cell-stage embryos). Each batch originated from at least three different rabbit couples. For each stage, three replicates were conducted. Total RNA was extracted as previously described and divided into two equal parts. One half was used for a single-round in vitro transcription of antisense RNA (aRNA) with the MessageAmp aRNA Kit (Ambion, Austin, TX) according to manufacturer's instructions. The second half was used for "global RT-PCR" amplification according to the protocol described by Pacheco-Trigon et al. (28). Indeed, we observed that the use of two independent amplification procedures makes it possible to detect a greater number of differentially expressed genes by an ANOVA analysis that takes the amplification method into account (L. C. Bui, unpublished observation). Each repeat was amplified according to both methods, with one repeat of each stage being amplified at the same time in order to minimize potential technical bias.

Labeling and microarray hybridization. Prehybridization of the microarrays was performed in 12-ml glass tubes with 1 ml of ExpressHyb Hybridization Solution (Clontech) at 68°C over 44 h.

An Atlas SMART Probe Amplification Kit (Clontech) and [α-^{33}P]ATP (Perkin Elmer, Waltham, MA) were used to label 500 ng of cDNA from the global RT-PCR. Five hundred nanograms of aRNA were reverse transcribed and [α-^{33}P]ATP labeled as described by Decraene et al. (10). Unincorporated nucleotides were eliminated by passage through a 1-ml G50-Sephadex column. Labeled targets recovered in a 50-μl final volume were added to the prehybridization solution. Hybridization was performed at 68°C for 24 h. Membranes were washed four times in 2× SSC, 1% SDS at 68°C for 30 min and once in 0.1× SSC, 0.5% SDS at 68°C for 30 min . Microarrays were then exposed to a phosphoscreen (IP plate, FujiFilm) for 20 h and scanned on a Fuji BAS 5000 phosphorimager. Hybridization signals were quantified with AGScan software (http://mulcyber.toulouse.inra.fr/gf/project/agscan).

Statistical analysis. After quantification, hybridization signals were log transformed and normalized before data analysis. All data sets are accessible in the NCBI Gene Expression Omnibus database (experimental series GSE12084). Differential analysis was performed by ANOVA with GenAnova software (11). For each array probe, the equation used for ANOVA was the following: $Y_{ijk} = \mu + S_i + M_j + R_k + \varepsilon_{ijk}$, where Y_{ijk} is array probe intensity; μ is the mean of intensities of expression measured for the probe; S_i, M_j, and R_k are the effects of the analyzed stage *i*, the amplification method *j*, and the biological repetition *k*, respectively; and ε_{ijk} is the residual error including all interactions between these factors.

Hierarchical clustering. To classify our different "conditions," unsupervised hierarchical clustering was performed with Multiexperiment Viewer (TMeV) software from the TM4 suite (http://www.tm4.org/mev.html).

Functional analysis of the rabbit embryo transcriptome. Functional interpretation of the microarray data was performed based on the Gene Ontology (GO) consortium annotation categories GO biological process, GO molecular function, and GO cellular component with the GeneTools web service (www.genetools.no). This software was chosen because it allows input of a gene reporter list (in our case Unigene cluster ID) without any specification concerning the species, which made it possible to take into account information obtained either from human or from mouse data banks. This resulted in a higher number of annotated sequences. Moreover, GeneTools (2) not only finds over- or underrepresented GO categories in a defined list of genes, comparing them to all the GO categories represented on the microarray, but also permits a direct comparison of two candidate gene lists, which is particularly interesting when performing a gene expression profile cluster-based comparison.

Real time RT-PCR. RNA was extracted from batches of 40 in vivo-developed embryos at the four-cell, early morula (20–30 cell), and blastocyst stages as described above. cDNAs were synthesized

from total RNA extracted from the 40 embryos with the Superscript III enzyme (Invitrogen) and random primer hexamers (Roche Diagnostics, Meylan, France) in a 20-μl final volume. The RT reaction was diluted to 400 μl in water. Each RT reaction was used to quantify the six candidate genes.

A PCR mix was prepared for each gene as follows: 12.5 μl of 2× Sybr Green Mastermix (Applied Biosystems, Courtaboeuf, France), 0.25 μl of uracil *N*-glycosylase (1 U/μl), 0.5 μl of each primer (10 μM initial concentration), 1.25 μl of H$_2$O, 10 μl for each diluted RT reaction. For each sample the PCR reaction was carried out in triplicate and the mean threshold cycle was determined. The thermal cyclic profile started with a 2-min step at 50°C, followed by 10 min at 95°C and 45 cycles of 95°C denaturation for 15 s, 60°C annealing and extension for 60 s. The reactions were performed on an ABI Prism 7000 sequence detector (Applied Biosystems). Dissociation curves were performed after each PCR run to ensure that a single PCR product had been amplified. A standard curve consisting in 10-fold dilution series of quantified amplicon was included in each run. Experiments were carried out three times starting from distinct batches of embryos. The three samples corresponding to the different embryo stages and making one repetition were extracted, reverse transcribed, and PCR amplified simultaneously. Gene expression data were thus obtained first per embryo equivalent whatever the stage. However, because of the huge increase in cell number and total RNA content between the early morula and the blastocyst stage, such a quantification can result in an increase in amounts despite the fact that the real expression per cell is unchanged (or even perhaps decreased). For this reason, and because the transcriptome results were obtained by hybridizing constant amounts of labeled cDNAs regardless of stage, we normalized the real-time quantitative RT-PCR (qRT-PCR) results to express them relative to a constant amount of total messenger RNA whatever the stage. This was done by dividing at each stage the estimated number of transcript copies by the amount of total messenger RNA.

RESULTS AND DISCUSSION

Construction of rabbit cDNA array dedicated to early embryonic development. To obtain a first-generation cDNA array dedicated to the rabbit preimplantation embryo, we focused on two gene categories: those expressed by the genome just after EGA and those expressed once FD events have resulted in a blastocyst. We therefore combined a PCR amplification of all the cDNA and a SSH strategy to construct two independent subtracted libraries enriched in EGA and FD transcripts, respectively. The EGA library was obtained by subtracting the latest pre-EGA stage (4-cell stage) embryo cDNAs from the earliest post-EGA stage (20- to 30-cell early morulae) cDNAs. Similarly, the FD library was obtained by subtracting predifferentiation-stage (late morulae) cDNAs from early postdifferentiation-stage (blastocyst stage) cDNAs. Such subtracted libraries, obtained from small amounts of starting RNA, have been shown to contain very scarce transcripts despite a normalization efficiency that varies with the initial abundance of the transcripts (6). For this reason, and also because early morulae and blastocysts express common genes, we applied a two-step sequencing strategy to both of these libraries before selecting candidate genes to include in our array. A first set of 1,920 clones from the FD library were sequenced. PCR inserts corresponding to 1,550 "high-quality" sequences of this set were then further hybridized to another set of 4,608 FD library clones, and to 4,608 EGA library clones, in order to select negative clones and eliminate positive redundant clones. From these two sets of FD and EGA library clones, 960 and 2,400
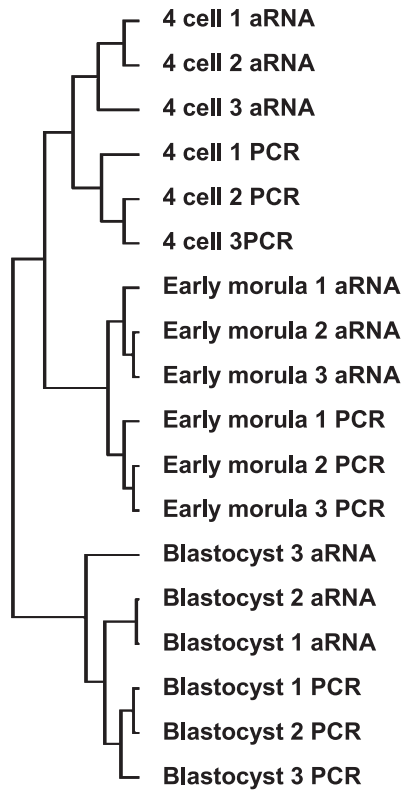
Fig. 1. Hierarchical clustering analysis of the 18 experimental conditions involving all the genes present on the array. aRNA, antisense RNA.

negative clones, respectively, were selected and sequenced, from which 856 and 2,029 "high-quality" sequences were obtained.

These sequences were then assembled with the available public rabbit ESTs into 2,022 contigs, of which 982 contain only EGA ESTs, 937 contain only FD ESTs, and only 103 contain both EGA and FD ESTs. The reduced size of this last category of contigs confirms the interest of the two-step sequencing strategy we developed. Because ESTs were obtained by SSH, their size varies between 150 and 800 bp. For each contig, the longest EST was chosen as the best representative. PCR inserts of the corresponding clones were synthesized and spotted onto nylon micromembranes, thus resulting in the first 2,022-"unique contig" rabbit array.

Embryo transcriptome analysis. To analyze gene regulation at EGA and during the FD events we screened the new rabbit embryo dedicated array with cDNA complex targets corresponding to early (20–30 cell) morulae, considered as an early post-EGA stage, and blastocyst-stage embryos. Since transcripts of maternal and embryonic origin coexist at these early stages, we included four-cell-stage embryo cDNAs in our screening because they represent the last stage containing the persistent maternal inheritance just before EGA. This additional stage thus provided information about the origin of the transcripts.

Embryos from at least three different rabbit couples were pooled in each sample to avoid any maternal or paternal effect on gene expression. Three biological replicates per stage were performed, each corresponding to a different pool of embryos. For each biological sample, RNA was extracted and divided

into two equal parts. Each part was subjected to one amplification method: RT-PCR amplification of all the cDNAs or in vitro transcription of aRNA to obtain the target material. A total of 18 hybridizations were performed (6 for each stage corresponding to 3 biological repeats each amplified by 2 different methods).

A hierarchical clustering of the experimental conditions was performed (Fig. 1). This clustering clearly individualized each of the three embryonic stages. Within each stage, the two amplification methods were then separated, evidencing an expected amplification method effect. The four-cell embryos and early morulae were grouped together, thus giving to the blastocyst stage a particular position regarding the expression of the genes present on the array. Interestingly, however, the blastocyst-to-early morula distance was greater than the blastocyst-to-four cell distance, indicating that the embryo transcriptome displayed transient properties at EGA.

To get more precise insight into the relationship between two successive stages, we performed a pairwise comparison of gene expression data for the three stages. Four hundred fifty-three and 505 genes were found differentially expressed [paired t-test, false discovery rate (FDR) $< 0.05\%$] between four-cell and early morula stages and between early morula and blastocyst stages, respectively (Fig. 2). Among these differentially expressed genes, 262 genes (58.3%) displayed an increased expression between the four-cell and early morula stages, reflecting the expected increase in transcription at EGA, while only 200 genes (39.8%) showed an increased expression between the early morula and blastocyst stages. According to this screening, the proportion of genes whose expression increased was thus significantly higher during EGA than during the appearance of the first differentiations ($P < 10^{-7}$, χ^2-test). For a majority of the genes differentially expressed between the early morula and blastocyst stages (60.2% according to our screening), the amount of transcripts thus decreased between these two stages. Such a decrease might result either from the degradation of maternal transcripts or from an early downregulation of embryonic gene transcription. To distinguish both
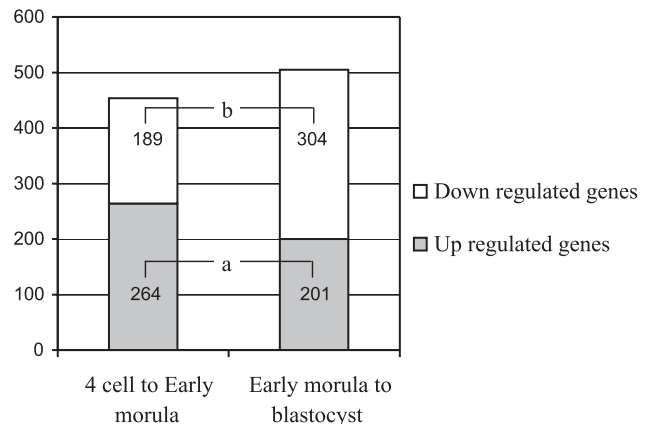
Fig. 2. Up- and downregulated genes between 2 consecutive stages. Histogram shows the numbers of differentially expressed genes between 2 consecutive stages according to paired t-test with false discovery rate (FDR) correction ($P < 0.05$) and their distribution into up- and downregulated genes. Proportions of up- and downregulated genes are significantly different during the transitions from 4-cell to early morula stage and from early morula to blastocyst stage ([a]$P < 0.002$ and [b]$P < 10^{-7}$ for up- and downregulated genes, respectively).

possibilities and to obtain information about the expression changes of individual genes during preimplantation development, we performed a supervised nonhierarchical clustering with the K-means method (TmeV software).

Expression profiles of individual genes. This clustering was performed for the subgroup of 1,176 genes displaying a "stage effect" with an FDR threshold of 0.10 when analyzed by ANOVA. These 1,176 genes were divided by the supervised nonhierarchical clustering into seven clusters that will be referred to hereafter by a combination of three letters: H, L, and M for high, low, and medium describing the relative level of expression of the genes in the cluster at the four-cell, early morula (20–30 cell), and blastocyst stages, respectively (Fig. 3).

We first validated this clustering in two different ways, comparing for some genes the pattern of expression obtained in this clustering with the profile established in a previous study (28) and comparing the clustering data with qRT-PCR results for six other candidate genes.

We previously had characterized in the rabbit embryo two categories of genes that displayed either transient or long-term induced expression at EGA. This distinction was founded on their different behavior between the 8- to 16-cell stage and the late morula stage: a decrease in expression was observed for transiently expressed genes, whereas an increase in expression was observed for long-term induced genes (28). We first validated the clustering by comparing the results of this previous characterization with those obtained in the present large-scale analysis for eight genes that are common to both analyses (Fig. 4). For those genes previously described as transiently expressed at EGA (SAMDC, clone 1, clone 8, clone 22, and clone 27), the patterns obtained in the present analysis approximately confirmed the transient expression at EGA. Small differences due to differences in the number and the exact timing of embryo stages were revealed in each study (only 3 stages were taken into account in the present analysis, and the early morula stage of the present study was flanked by the 8- to 16-cell and late morula stages analyzed in the previous analysis). The present study also confirmed the progressive increase in transcript accumulation for the genes previously described as "long-term induced" (ribl7, Uba80, and clone 72). Their rate of accumulation, however, might display some differences according to the study (see, for example, ribl7), which were probably caused by the use of two amplification methods in the present analysis. Based on the results obtained using these eight candidate genes, we concluded that our present results are valid.
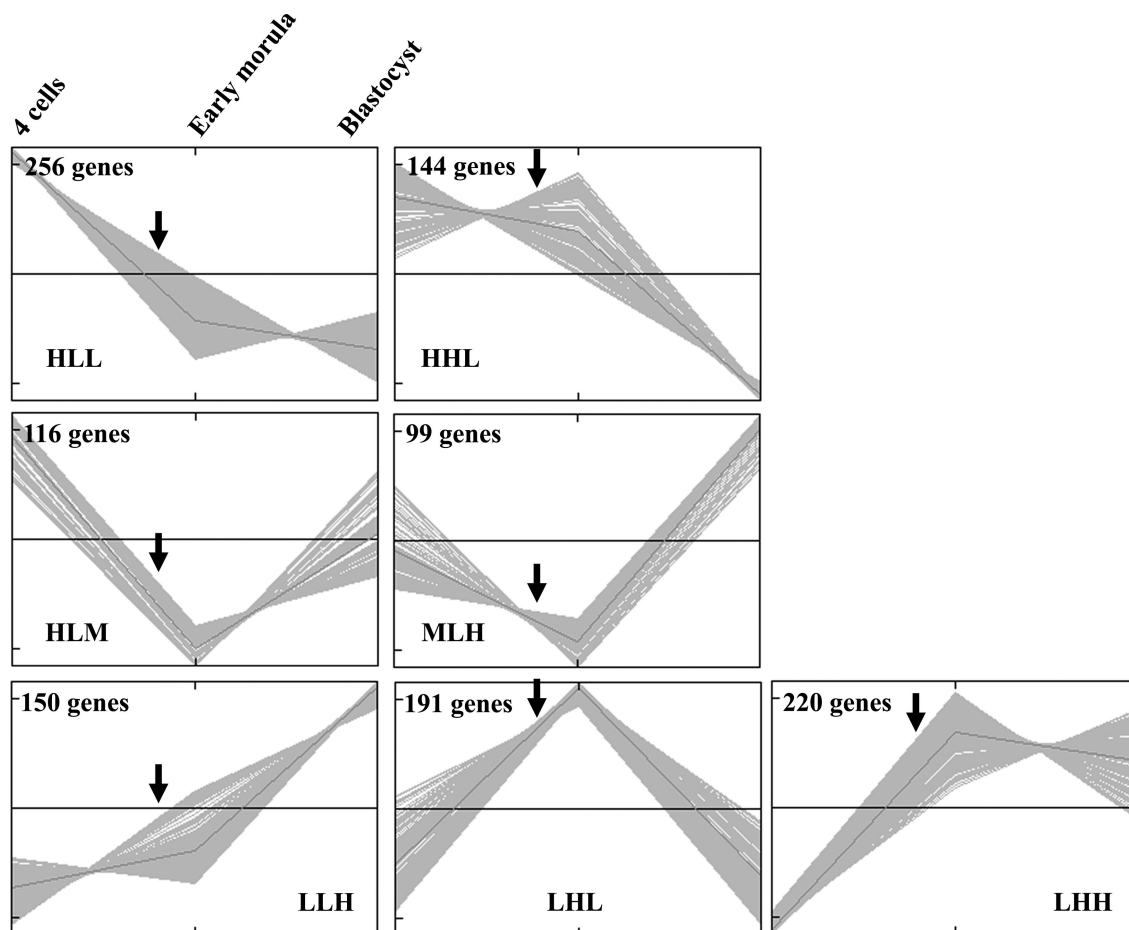
Fig. 3. Time course analysis of individual genes. The 1,176 genes with a stage effect (ANOVA with FDR correction <0.10) were dispatched into 7 clusters by a K-means nonhierarchical clustering method. The mnemonic description of these clusters relies on a combination of 3 letters: H, L, and M for high, low, and medium, describing the relative level of expression of the genes in the cluster at the 4-cell, early morula (20–30 cell), and blastocyst stages, respectively. Arrows indicate embryonic genome activation at the 8- to 16-cell stage.
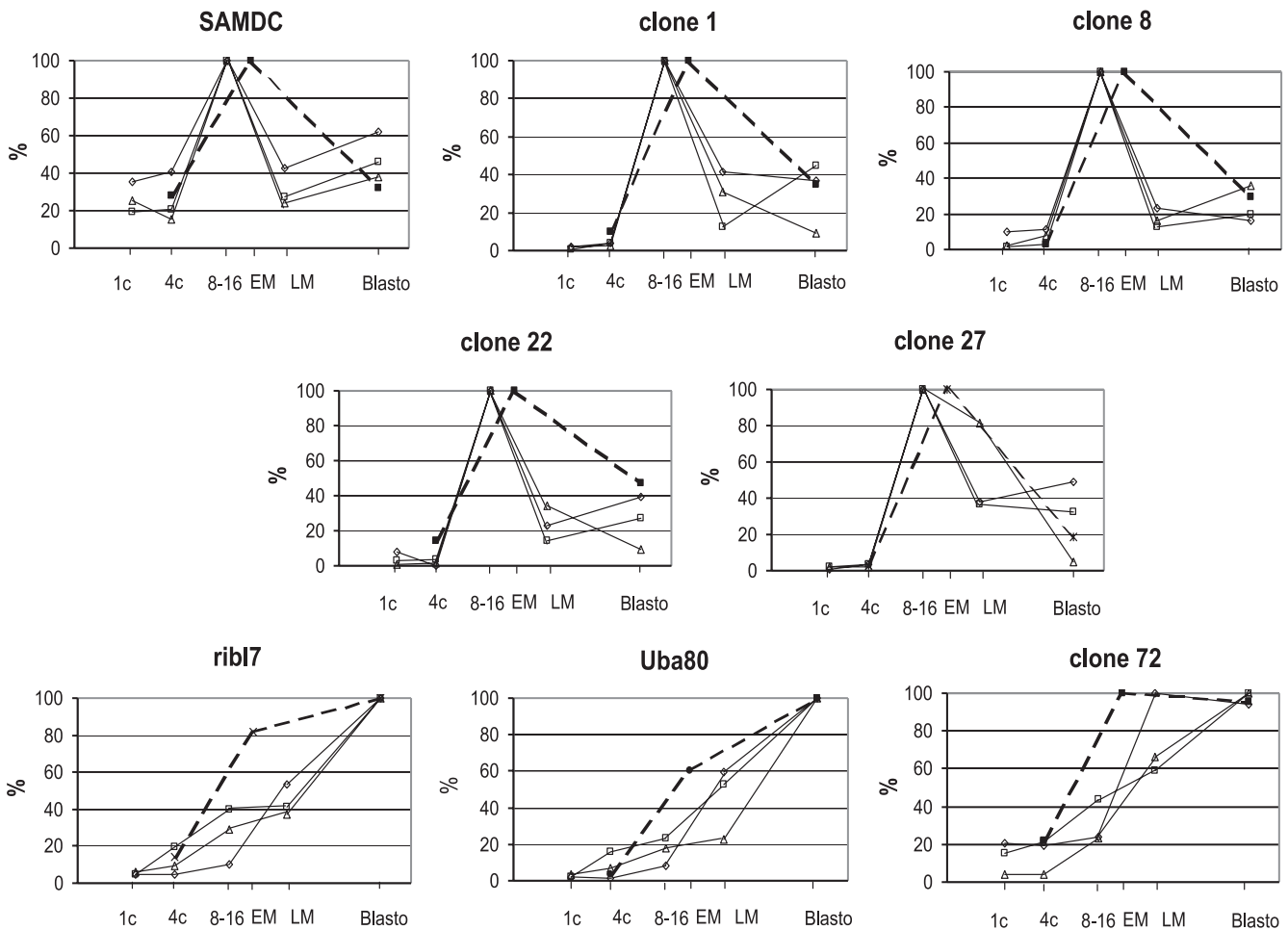
Fig. 4. Validation of microarray data by comparison with patterns of expression previously established for 8 clones. Expression profiles obtained from the microarray data (mean of 6 hybridizations per stage: 3 biological repetitions and 2 amplification methods) are shown as dashed lines. In microarray experiments expression levels were assessed in 4-cell embryos [4c, 32 hours postcoitum (hpc)], early morulae (EM, 58 hpc), and blastocysts (Blasto, 100 hpc). Solid lines represent expression profiles previously characterized for these clones (28). In the previous analysis expression levels were assessed in zygotes (1c, 19 hpc), 4-cell (4c, 32 hpc), 8- to 16-cell embryos (8–16, 50 hpc), late morulae (LM, 69 hpc), and blastocysts at 100 hpc; each line represents 1 repetition of the quantification experiment. Expression levels are expressed as % of maximal expression value detected for the clone.

Another way to validate the clustering results was to analyze by qRT-PCR the expression patterns of six additional candidate genes that belong to three different clusters (clusters HLL, LHL, and LHH). We choose to analyze both identified and unidentified genes (see Table 1). RNAs were extracted from pools of 40 in vivo developed embryos. Three independent pools were used at each stage (4 cells, 20- to 30-cell early morulae, and blastocyst stage) to provide three independent repetitions of the quantifications. Each pool of embryos was used to quantify the transcripts of the six candidate genes

Table 1. *Identification of candidate genes analyzed by qRT-PCR and sequence of corresponding primers*

cDNA Clone Name	Gene Identification	Primer Sequence
lcao0043e06	Unknown	Forward: GCAGCAGATTTTAGGAAACGA
		Reverse: GGGTGCAAACCAAGAACACT
lcap0024 h10	Unknown	Forward: GGGGAGCTAGGAGAGCAAAC
		Reverse: CAAACCCTCATCCATCATCC
lcap0010c03	Tudor KH domain containing protein mRNA	Forward: AACATGGATGCGTTCTTTCC
		Reverse: TTTTCCTGAGTTTCCTCTCTCCT
lcao0026 h06	t Complex protein 1 mRNA	Forward: CTTTCACTATGGTTGGCTCAAA
		Reverse: GTTGAGAGCTTTTCACAATGAGG
lcao0041 g07	Unknown	Forward: CGCATTAAGAGAGCACTGGAC
		Reverse: TTTCCCGAATAACCTCTTTCAG
lcao0048d05	Unknown	Forward: CGGGATTGTTTTAGTCTTGGAAGTA
		Reverse: AGCTTGTATTTAGCTGCGATGC

qRT-PCR, quantitative real-time RT-PCR.

Fig. 5. Validation of the microarray data by quantitative real-time RT-PCR (qRT-PCR). Expression profiles of 6 candidate genes belonging to 3 different clusters (HLL, LHL, and LHH) were assessed by qRT-PCR. Three repetitions were performed starting from total RNA extracted from 3 different batches of 40 embryos at each of the 3 stages involved in the clustering. Total RNAs from 1 equivalent embryo were used for qRT-PCR with designed primers. Since messenger RNAs hugely increase at blastocyst stage in the rabbit, qRT-PCR values e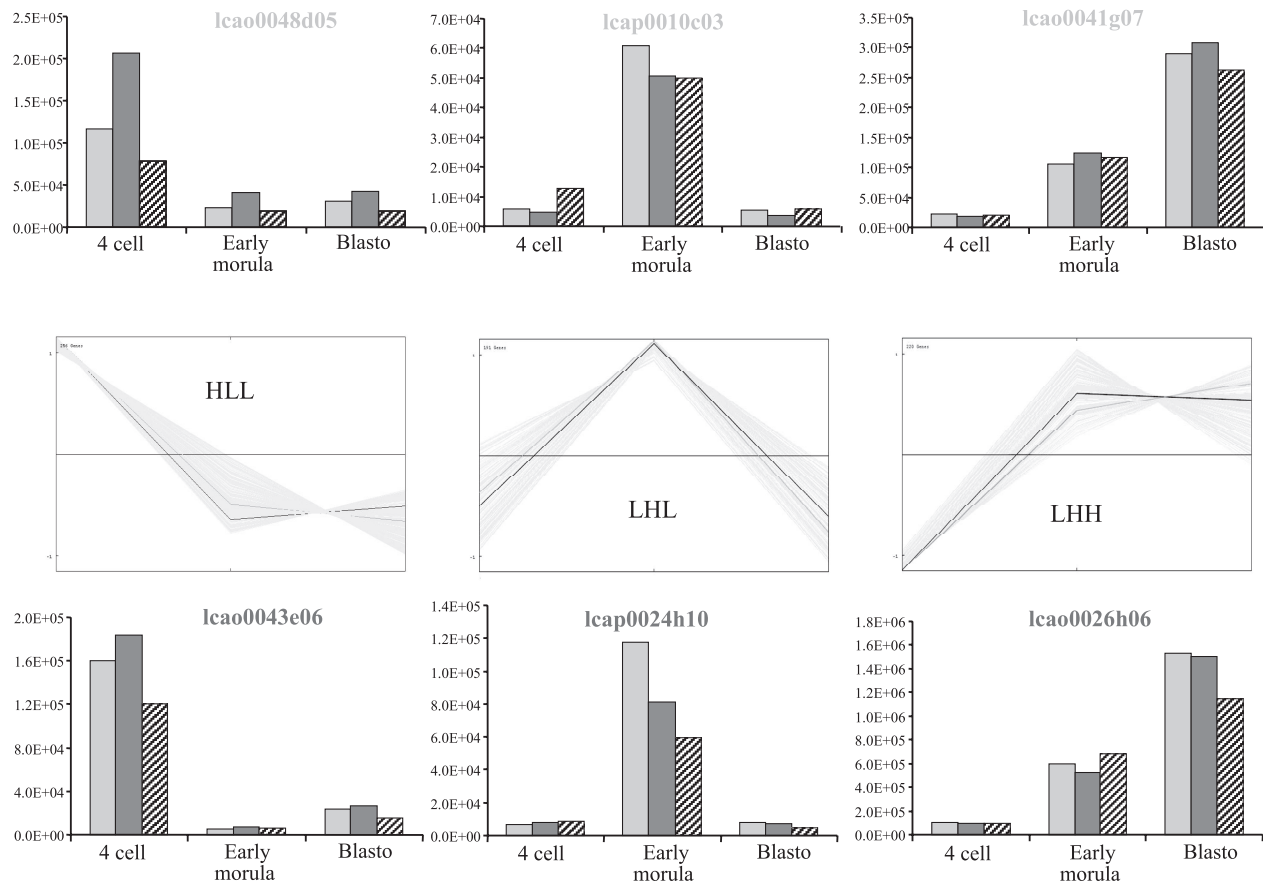xpressed in number of copies of the candidate transcript were normalized to relate them to a constant amount of mRNA whatever the stage (see details in the text). Dark gray and pale gray lines in each cluster represent the 2 gene profiles according to the microarray data. Their corresponding qRT-PCR results are represented on both sides.

starting from one equivalent embryo per stage. The rough qRT-PCR results showed an apparent overexpression of the transcripts at the blastocyst stage compared with the large-scale transcriptomic analysis results (data not shown). In the rabbit embryo, however, the total amount of poly(A) RNA increased hugely at the blastocyst stage [~13 times more total poly(A) RNA at the blastocyst stage than at the previous stages] (12). Since the transcriptome results were obtained by hybridizing constant amounts of labeled cDNAs whatever the stage, we normalized the qRT-PCR results to express them relative to a constant amount of total messenger RNA whatever the stage; this was done by dividing at each stage the estimated number

of transcript copies by the amount of total messenger RNA. In these conditions we observed a good correlation between qRT-PCR results and transcriptomic results for each candidate gene (Fig. 5). The initial discrepancies between both kinds of analysis was thus due to the relative underloading of the blastocyst sample in the transcriptome analysis, as discussed by Su et al. (32). We thus concluded that our transcriptome analysis properly described the relative quantities of transcripts in a constant amount of total messenger RNAs all over preimplantation development.

Clusters HLL and HHL represented genes whose maternal transcripts were still abundant at the four-cell stage compared

Table 2. *Distribution of up- and downregulated genes among clusters*

		n	Cluster HLL	Cluster LLH	Cluster HHL	Cluster LHL	Cluster HLM	Cluster LHH	Cluster MLH
Stage effect*		1,176	256	150	144	191	116	220	99
4-Cell to early morula†	↗	264	0	13 (4.9)	0	93 (35.2)	0	158 (59.8)	0
4-Cell to early morula†	↘	181	110 (60.8)	0	7 (3.8)	0	51 (28.2)	0	13 (7.2)
Early morula to blastocyst†	↗	201	0	98 (48.8)	0	0	30 (14.9)	2 (0.01)	71 (35.3)
Early morula to blastocyst†	↘	268	28 (10.4)	0	90 (33.6)	132 (43.4)	0	18 (6.7)	0

Data are total number of genes (n), upregulated (↗) and downregulated (↘) genes between the consecutive embryo stages, and their distribution among the 7 clusters [number (percentage)]. The 1,176 genes with a stage effect in ANOVA were taken into account. L, low, M, medium, H, high expression. *ANOVA with false discovery rate (FDR) correction ($P < 0.1$); †paired t-test with FDR correction ($P < 0.05$).

Table 3. *Examples of representative genes in each cluster+*

Cluster HLL	
Ldha	Lactate dehydrogenase C
Vdac3	Voltage-dependent anion channel 3
TOP2A	Topoisomerase (DNA) IIα 170 kDa
DDB1	Damage-specific DNA binding protein 1, 127 kDa
NONO	NonPOU domain containing, octamer-binding
SDCBP	Syndecan binding protein (syntenin)
Lars2	Leucyl-tRNA synthetase, mitochondrial
Ccar1	Cell division cycle and apoptosis regulator 1
CTH	Cystathionase (cystathionine γ-lyase)
COPG	Coatomer protein complex, subunit γ
Map2k1ip1	Mitogen-activated protein kinase kinase 1 interacting protein 1
SAT1	Spermidine/spermine N1-acetyltransferase 1
STRBP	Spermatid perinuclear RNA binding protein
ITGB1	Integrin, β1
MAGOH	Mago-nashi homolog, proliferation-associated (*Drosophila*)
SLC7A7	Solute carrier family 7 (cationic amino acid transporter), member 7
Ing3	Inhibitor of growth family, member 3
Igfbp7	Insulin-like growth factor binding protein 7
SLC20A1	Solute carrier family 20 (phosphate transporter), member 1
Ing3	Inhibitor of growth family, member 3
Cluster LLH	
DDX3X	DEAD (Asp-Glu-Ala-Asp) box polypeptide 3, X-linked
Slc6a8	Solute carrier family 6 (creatine transporter), member 8
Pdhb	Pyruvate dehydrogenase (lipoamide) β
GDF3	Growth differentiation factor 3
Cox7c	Cytochrome-*c* oxidase, subunit VIIc
FBP1	Fructose-1,6-bisphosphatase 1
AHCY	*S*-adenosylhomocysteine hydrolase
ECT2	Epithelial cell transforming sequence 2 oncogene
COX7B	Cytochrome-*c* oxidase subunit VIIb
EIF5	Eukaryotic translation initiation factor 5
Eef1a1	Eukaryotic translation elongation factor 1 α1
Serinc1	Serine incorporator 1
Hspa5	Heat shock 70-kDa protein 5 (glucose-regulated protein)
Hspd1	Heat shock protein 1 (chaperonin)
Mthfd1	Methylenetetrahydrofolate dehydrogenase
UBE1	Ubiquitin-activating enzyme E1
GPHN	Gephyrin
LOC440567	Similar to Ubiquinol-cytochrome *c* reductase complex 11 kDa
MYC	V-myc myelocytomatosis viral oncogene homolog (avian)
NFX1	Nuclear transcription factor, X-box binding 1
Cluster HHL	
AMD1	Adenosylmethionine decarboxylase 1
Ybx1	Y box protein 1
Eif4a1	Eukaryotic translation initiation factor 4A1
HLA-DQA1	Major histocompatibility complex, class II, DQ α1
LEPR	Leptin receptor
Naca	Nascent polypeptide-associated complex α polypeptide
PAPOLA	Poly(A) polymerase α
SON	SON DNA binding protein
Prpf8	Pre-mRNA processing factor 8
PABPC4	Poly(A) binding protein, cytoplasmic 4
DPPA5	Developmental pluripotency associated 5
CDC2	Cell division cycle 2, G$_1$ to S and G$_2$ to M
UBL5	Ubiquitin-like 5
SFRS11	Splicing factor, arginine/serine-rich 11
CENPI	Centromere protein I
Sfrs1	Splicing factor, arginine/serine-rich 1
HNRPF	Heterogeneous nuclear ribonucleoprotein F
CNOT6	CCR4-NOT transcription complex, subunit 6
PRMT6	Protein arginine methyltransferase 6
ATR	Ataxia telangiectasia and Rad3 related

Continued

Table 3.—*Continued*

Cluster LHL	
SLC19A3	Solute carrier family 19, member 3
Polr2 g	Polymerase (RNA) II (DNA directed) polypeptide G
Eif3 s2	Eukaryotic translation initiation factor 3, subunit 2 (β)
SAP18	Sin3A-associated protein, 18 kDa
TFRC	Transferrin receptor (p90, CD71)
NPM1	Nucleophosmin
H2afz	H2A histone family, member Z
SMS	Spermine synthase
MAT2A	Methionine adenosyltransferase II, α
Triap1	TP53 regulated inhibitor of apoptosis 1
NP	Nucleoside phosphorylase
MED18	Mediator of RNA polymerase II transcription, subunit 18 homolog
LIN28	Lin-28 homolog (*C. elegans*)
CDC23	CDC23 (cell division cycle 23, yeast, homolog)
CDC6	CDC6 cell division cycle 6 homolog (*S. cerevisiae*)
HUWE1	HECT, UBA and WWE domain containing 1
LOC667250	Similar to H3 histone, family 3B
GPBP1	GC-rich promoter binding protein 1
DDAP2	Developmental pluripotency associated 2
SCNM1	Sodium channel modifier 1
Cluster HLM	
SOD1	Superoxide dismutase 1, soluble
Hsp90b1	Heat shock protein 90 kDa β member 1
CS	Citrate synthase
SF3A3	Splicing factor 3a, subunit 3, 60 kDa
PDCD8	Programmed cell death 8
Atp5j	ATP synthase, H$^+$ transporting, mitochondrial F$_0$ complex, subunit F
TLN2	Talin 2
MAPK9	Mitogen-activated protein kinase 9
IARS	Isoleucine-tRNA synthetase
Arf1	ADP-ribosylation factor 1
QRSL1	Glutaminyl-tRNA synthase-like 1
Prpf8	Pre-mRNA processing factor 8
USP16	Ubiquitin-specific peptidase 16
PSMD2	Proteasome 26S subunit, nonATPase, 2
PDCD10	Programmed cell death 10
USP7	Ubiquitin specific peptidase 7
POLK	Polymerase (DNA directed) κ
Pparg	Peroxisome proliferator-activated receptor γ
Trip12	Thyroid hormone receptor interactor 12
RAB30	RAB30, member RAS oncogene family
Cluster LHH	
VDAC2	Voltage-dependent anion channel 2
RPL36AL	Ribosomal protein L36a-like
RPS24	Ribosomal protein S24
NAP1L1	Nucleosome assembly protein 1-like 1
Rps6	Ribosomal protein S6
Eif3 s12	Eukaryotic translation initiation factor 3, subunit 12
Hspa4	Heat shock protein 4
Timm17a	Translocase of inner mitochondrial membrane 17a
PABPC1	Poly(A) binding protein, cytoplasmic 1
NDUFB3	NADH dehydrogenase (ubiquinone) 1β subcomplex, 3, 12 kDa
HDAC1	Histone deacetylase 1
Atp5b	ATP synthase, H$^+$ transporting mitochondrial F$_1$ complex, β subunit
GFM1	G elongation factor, mitochondrial 1
GTF2F2	General transcription factor IIF, polypeptide 2, 30 kDa
POLR2H	Polymerase (RNA) II (DNA directed) polypeptide H
Gtf2e1	General transcription factor II E, polypeptide 1 (α subunit)
SENP2	SUMO1/sentrin/SMT3 specific peptidase 2
TOMM7	Translocase of outer mitochondrial membrane 7 homolog (yeast)
SLC7A3	Solute carrier family 7 (cationic amino acid transporter), member 3
Pgk1	Phosphoglycerate kinase 1

Continued

Table 3.—*Continued*

Cluster MLH

Hsp90ab1	Heat shock protein 90 kDa α (cytosolic), class B member 1
ATP5H	ATP synthase, H^+ transporting, mitochondrial F_0 complex, subunit d
Hif1a	Hypoxia inducible factor 1, α subunit
CA2	Carbonic anhydrase II
EPB41L3	Erythrocyte membrane protein band 4.1-like 3
CD53	CD53 molecule
ATP5O	ATP synthase, H^+ transporting, mitochondrial F1 complex, O subunit
TNC	Tenascin C (hexabrachion)
MYO1E	Myosin IE
Ndufa9	NADH dehydrogenase (ubiquinone) 1α subcomplex, 9
KPNA4	Karyopherin alpha 4 (importin α3)
GALM	Galactose mutarotase (aldose 1-epimerase)
Pdhb	Pyruvate dehydrogenase (lipoamide) β
CD44	CD44 molecule (Indian blood group)
ASNSD1	Asparagine synthetase domain containing 1
RHOT1	Ras homolog gene family, member T1
KRT18	Keratin 18
Nasp	Nuclear autoantigenic sperm protein (histone-binding)
SMEK2	SMEK homolog 2, suppressor of mek1 (*Dictyostelium*)
Stt3a	STT3, subunit of the oligosaccharyltransferase complex, homolog A (*S. cerevisiae*)

with post-EGA stages. Cluster HLL gathered genes whose maternal transcripts were rapidly degraded between the four-cell and EGA stages, while cluster HHL gathered genes whose maternal transcript degradation was delayed until after the onset of embryonic transcription. The presence of such maternally expressed genes on our array dedicated to EGA and FD may result from defaults in subtraction efficiency when transcripts are abundant in both tester and driver material as described in our previous validation of SSH libraries obtained from early embryos (6). Clusters HLM and MLH regrouped genes whose transcripts were inherited from the oocyte at the four-cell stage, but were highly reexpressed from the embryonic genome as soon as EGA. Both of these clusters differed from the relative abundance of maternally inherited transcripts still present at the four-cell stage and embryonic transcripts already accumulated at the blastocyst stage. Maternally inherited transcripts were predominant for cluster HLM genes, whereas they were less abundant than embryonic transcripts for cluster MLH genes. Clusters LLH, LHL, and LHH represented genes whose transcripts were scarce in the maternal inheritance at the four-cell stage and were hugely transcribed from the embryonic genome during the four cell-to-blastocyst period. These genes were dispatched between the three clusters according to both the stage of initiation of their transcription, EGA for cluster LHL and LHH or mainly post-EGA for cluster LLH, and the duration of their transcription period: "long-lasting" transcription for clusters LLH and LHH vs. abrupt and transient expression for cluster LHL.

To answer the question of the maternal or embryonic origin of the predominant gene downregulation evidenced after EGA, we investigated how downregulated genes were distributed across the different clusters (Table 2). Among the 1,176 genes dispatched in the 7 clusters, 268 genes were detected as downregulated between the early morula stage and the blastocyst stage ($P < 0.05$, paired t-test with FDR correction), only 118 (28 + 90), or 44% (118/268), of which belonged to clusters HLL and HHL. These were maternally inherited tran-

scripts still in course of degradation after EGA. Embryonically transcribed genes thus significantly took part [56%, (132 + 18)/268] in the broad downregulation we showed after EGA, and most of these embryonically transcribed genes belonged to cluster LHL (transiently expressed at EGA, then abruptly downregulated). Their expression pattern was thus greatly responsible for the transient properties of EGA transcriptome evidenced by the hierarchical clustering of our hybridization experiments.

Functional evolution of embryo transcriptome from pre-EGA to FD stages. We looked for the identity of genes in each cluster and for their functional significance. Therefore, we blasted the sequences of the 2,022 contigs containing the ESTs present on the array against the human and mouse genomes and retained the significant results ($E < 10^{-30}$; see MATERIALS AND METHODS). With this threshold, 65% of the genes present on our array were identified and could be associated to a GO functional annotation. Table 3 gives examples of genes belonging to each of the seven clusters. We then performed an automated ontological analysis using the GeneTools web service (2). Table 4 gives a representative view of the GO categories over- or underrepresented in each cluster compared with those of the whole microarray. The most significant functions among these are pointed out thereafter, keeping, however, their diversity because it reflected the highly dynamic properties of the transcriptome at these early stages.

The main overrepresented biological processes in cluster HLL were "nitrogen compound metabolism," "tRNA metabolism," "amino acid and derivative metabolism," and "intracellular signaling cascade," while transcripts involved in "regulation of transcription, DNA dependent" were underrepresented among these pre-EGA eliminated maternal transcripts. Genes involved in "biopolymer metabolism" and "energy reserve metabolism" were overrepresented in cluster HHL. In this cluster, "RNA metabolism" and "RNA processing" were also overrepresented. This suggested a delay in the degradation of maternal transcripts involved in these functions, making them available for the processing of the first embryonically encoded transcripts at EGA.

The most overrepresented genes in cluster HLM were involved in protein degradation, as exemplified by biological processes "proteolysis" and "ubiquitin cycle," while cluster MLH gathered genes involved in "cytoskeleton-dependent intracellular transport," "nucleotide metabolism," and "ATP metabolism."

Genes involved in cell metabolism were overrepresented in cluster LLH, while the mostly overrepresented genes in cluster LHH encoded for protein biosynthesis. Besides genes involved in "nuclear mRNA splicing via spliceosome," cluster LHL displayed genes involved in "DNA integrity checkpoint," "mitosis," "DNA metabolism," and "nucleobase and nucleic acid metabolism." The corresponding genes were involved in "control of mitotic program via DNA replication checkpoints" (CDC23, CDC6, Cdc2a) and in "negative regulation of programmed cell death" (Triap1, TXNDC1, NPM1). Interestingly, a unique molecular function was found overrepresented in cluster LHL: "transferase activity, transferring alkyl or aryl groups." However, the functions encoded by those genes grouped in cluster LHL in development were more difficult to describe since this cluster displayed the highest proportion of unannotated sequences according to our annotation strategy.

Table 4. *Functional analysis of genes in the seven clusters*

GO	Name	GO Tree	All Genes	No. in Cluster	P Value	Over or Under
		Cluster HLL				
GO:0008150	Biological process	BP	582	92		
GO:0003674	Molecular function	MF	617	98		
GO:0006807	Nitrogen compound metabolism	BP	29	12	0.001	O
GO:0006418	tRNA aminoacylation for protein translation	BP	10	6	0.002	O
GO:0006519	Amino acid and derivative metabolism	BP	25	10	0.003	O
GO:0006399	tRNA metabolism	BP	13	6	0.009	O
GO:0007242	Intracellular signaling cascade	BP	33	11	0.011	O
GO:0009966	Regulation of signal transduction	BP	14	6	0.014	O
GO:0016049	Cell growth	BP	4	3	0.014	O
GO:0006695	Cholesterol biosynthesis	BP	4	3	0.014	O
GO:0007243	Protein kinase cascade	BP	11	5	0.019	O
GO:0009967	Positive regulation of signal transduction	BP	8	4	0.025	O
GO:0007154	Cell communication	BP	68	17	0.034	O
GO:0006281	DNA repair	BP	21	7	0.034	O
GO:0007267	Cell-cell signaling	BP	9	4	0.039	O
GO:0006355	Regulation of transcription, DNA-dependent	BP	89	7	0.026	U
GO:0031323	Regulation of cellular metabolism	BP	119	11	0.034	U
GO:0004812	Aminoacyl-tRNA ligase activity	MF	10	6	0.002	O
GO:0016410	*N*-acyltransferase activity	MF	5	3	0.031	O
GO:0003676	Nucleic acid binding	MF	175	17	0.007	U
GO:0003723	RNA binding	MF	70	4	0.014	U
GO:0005198	Structural molecule activity	MF	34	1	0.029	U
GO:0003735	Structural constituent of ribosome	MF	22	0	0.035	U
		Cluster LLH				
GO:0008150	Biological process	BP	582	43		
GO:0003674	Molecular function	MF	617	47		
GO:0006725	Aromatic compound metabolism	BP	2	2	0.005	O
GO:0006091	Generation of precursor metabolites and energy	BP	47	9	0.005	O
GO:0051188	Cofactor biosynthesis	BP	13	4	0.011	O
GO:0009108	Coenzyme biosynthesis	BP	13	4	0.011	O
GO:0044272	Sulfur compound biosynthesis	BP	3	2	0.015	O
GO:0006119	Oxidative phosphorylation	BP	14	4	0.015	O
GO:0006006	Glucose metabolism	BP	4	2	0.029	O
GO:0000096	Sulfur amino acid metabolism	BP	4	2	0.029	O
GO:0006730	One-carbon compound metabolism	BP	4	2	0.029	O
GO:0002245	Physiological response to wounding	BP	10	3	0.031	O
GO:0006118	Electron transport	BP	26	5	0.036	O
GO:0043283	Biopolymer metabolism	BP	192	7	0.017	U
GO:0016070	RNA metabolism	BP	78	1	0.020	U
GO:0015078	Hydrogen ion transporter activity	MF	16	5	0.005	O
GO:0016801	Hydrolase activity, acting on ether bonds	MF	2	2	0.006	O
GO:0005215	Transporter activity	MF	58	10	0.008	O
GO:0008324	Cation transporter activity	MF	26	6	0.010	O
GO:0016491	Oxidoreductase activity	MF	52	9	0.012	O
GO:0015075	Ion transporter activity	MF	31	6	0.024	O
GO:0004004	ATP-dependent RNA helicase activity	MF	4	2	0.031	O
GO:0008186	RNA-dependent ATPase activity	MF	4	2	0.031	O
GO:0015171	Amino acid transporter activity	MF	5	2	0.049	O
GO:0016740	Transferase activity	MF	80	1	0.021	U
		Cluster HHL				
GO:0008150	Biological process	BP	582	50		
GO:0003674	Molecular function	MF	617	52		
GO:0016070	RNA metabolism	BP	78	17	0.000	O
GO:0006396	RNA processing	BP	66	15	0.000	O
GO:0006397	mRNA processing	BP	42	10	0.002	O
GO:0043283	Biopolymer metabolism	BP	192	26	0.004	O
GO:0008380	RNA splicing	BP	41	9	0.005	O
GO:0006112	Energy reserve metabolism	BP	2	2	0.007	O
GO:0000398	Nuclear mRNA splicing, via spliceosome	BP	21	5	0.027	O
GO:0003723	RNA binding	MF	70	16	0.000	O
GO:0004888	Transmembrane receptor activity	MF	5	3	0.005	O
GO:0030515	snoRNA binding	MF	3	2	0.020	O
GO:0031420	Alkali metal ion binding	MF	8	3	0.023	O
		Cluster LHL				
GO:0008150	Biological process	BP	582	54		

Continued

Table 4.—*Continued*

GO	Name	GO Tree	All Genes	No. in Cluster	P Value	Over or Under
GO:0003674	Molecular function	MF	617	58		
GO:0031570	DNA integrity checkpoint	BP	3	3	0.001	O
GO:0006139	Nucleobase, nucleoside, nucleotide, and nucleic acid metabolism	BP	211	29	0.007	O
GO:0000398	Nuclear mRNA splicing, via spliceosome	BP	21	6	0.009	O
GO:0043170	Macromolecule metabolism	BP	299	36	0.022	O
GO:0000080	G_1 phase of mitotic cell cycle	BP	3	2	0.024	O
GO:0043069	Negative regulation of programmed cell death	BP	13	4	0.025	O
GO:0016765	Transferase activity, transferring alkyl or aryl (other than methyl) groups	MF	3	2	0.025	O
GO:0006259	DNA metabolism	BP	48	9	0.032	O
GO:0000087	M phase of mitotic cell cycle	BP	14	4	0.033	O
GO:0000278	Mitotic cell cycle	BP	15	4	0.042	O
	Cluster HLM					
GO:0008150	Biological process	BP	582	39		
GO:0003674	Molecular function	MF	617	42		
GO:0006508	Proteolysis	BP	27	6	0.006	O
GO:0006512	Ubiquitin cycle	BP	36	7	0.007	O
GO:0044257	Cellular protein catabolism	BP	13	4	0.008	O
GO:0016790	Thiolester hydrolase activity	MF	4	3	0.001	O
GO:0004221	Ubiquitin thiolesterase activity	MF	4	3	0.001	O
GO:0004843	Ubiquitin-specific protease activity	MF	4	3	0.001	O
GO:0043169	Cation binding	MF	107	15	0.003	O
GO:0046872	Metal ion binding	MF	123	16	0.004	O
GO:0008233	Peptidase activity	MF	22	5	0.013	O
GO:0005509	Calcium ion binding	MF	17	4	0.023	O
GO:0008270	Zinc ion binding	MF	75	10	0.026	O
	Cluster LHH					
GO:0008150	Biological process	BP	582	66		
GO:0003674	Molecular function	MF	617	70		
GO:0044249	Cellular biosynthesis	BP	102	23	0.000	O
GO:0006412	Protein biosynthesis	BP	72	21	0.000	O
GO:0044267	Cellular protein metabolism	BP	178	35	0.000	O
GO:0006414	Translational elongation	BP	4	3	0.005	O
GO:0051297	Centrosome organization and biogenesis	BP	2	2	0.013	O
GO:0043488	Regulation of mRNA stability	BP	2	2	0.013	O
GO:0051704	Interaction between organisms	BP	2	2	0.013	O
GO:0044237	Cellular metabolism	BP	422	56	0.019	O
GO:0006508	Proteolysis	BP	27	7	0.024	O
GO:0042254	Ribosome biogenesis and assembly	BP	17	5	0.034	O
GO:0006367	Transcription initiation from RNA polymerase II promoter	BP	3	2	0.035	O
GO:0005198	Structural molecule activity	MF	34	12	0.000	O
GO:0003735	Structural constituent of ribosome	MF	22	12	0.000	O
GO:0003746	Translation elongation factor activity	MF	3	3	0.001	O
GO:0008233	Peptidase activity	MF	22	7	0.008	O
GO:0008135	Translation factor activity, nucleic acid binding	MF	25	7	0.016	O
GO:0004298	Threonine endopeptidase activity	MF	6	3	0.022	O
GO:0042802	Identical protein binding	MF	16	5	0.026	O
GO:0015450	Protein translocase activity	MF	3	2	0.035	O
GO:0045182	Translation regulator activity	MF	29	7	0.036	O
GO:0016874	Ligase activity	MF	36	0	0.025	U
GO:0016301	Kinase activity	MF	32	0	0.040	U
	Cluster MLH					
GO:0008150	Biological process	BP	582	36		
GO:0003674	Molecular function	MF	617	38		
GO:0009607	Response to biotic stimulus	BP	14	4	0.008	O
GO:0030705	Cytoskeleton-dependent intracellular transport	BP	8	3	0.010	O
GO:0009117	Nucleotide metabolism	BP	16	4	0.013	O
GO:0015986	ATP synthesis coupled proton transport	BP	10	3	0.019	O
GO:0015985	Energy-coupled proton transport, down electrochemical gradient	BP	10	3	0.019	O
GO:0006754	ATP biosynthesis	BP	11	3	0.025	O
GO:0046034	ATP metabolism	BP	11	3	0.025	O
GO:0007010	Cytoskeleton organization and biogenesis	BP	20	4	0.029	O
GO:0009142	Nucleoside triphosphate biosynthesis	BP	12	3	0.033	O
GO:0009201	Ribonucleoside triphosphate biosynthesis	BP	12	3	0.033	O
GO:0006119	Oxidative phosphorylation	BP	14	3	0.049	O

Continued

Table 4.—*Continued*

GO	Name	GO Tree	All Genes	No. in Cluster	*P* Value	Over or Under
GO:0043283	Biopolymer metabolism	BP	192	6	0.042	U
GO:0004576	Oligosaccharyl transferase activity	MF	3	2	0.011	O
GO:0046961	Hydrogen-transporting ATPase activity, rotational mechanism	MF	10	3	0.019	O
GO:0019829	Cation-transporting ATPase activity	MF	11	3	0.025	O
GO:0003774	Motor activity	MF	12	3	0.032	O
GO:0016758	Transferase activity, transferring hexosyl groups	MF	5	2	0.033	O
GO:0003676	Nucleic acid binding	MF	175	2	0.001	U
GO:0003723	RNA binding	MF	70	0	0.015	U

Data are Gene Ontology (GO) categories from 2 branches of the GO tree (BP, biological process; MF, molecular function) overrepresented (O) or underrepresented (U) in each cluster. Lines without *P* value represent the total number of GO categories in a GO tree branch for the considered cluster.

While 65% of the genes present on the array were identified, this proportion was significantly lower for genes belonging to cluster LHL (57.6%; $P < 0.05$, χ^2-test) but significantly higher for cluster LHH (76.8%; $P < 0.001$, χ^2-test). The high proportion of still unknown genes in cluster LHL confirmed the interest in establishing dedicated arrays to analyze specific stages of embryo development. It also suggested that a high proportion of genes transiently expressed at EGA were involved in embryo-specific and still not precisely known events. This proportion was higher among genes transiently expressed at EGA (cluster LHL) than among those progressively transcribed from EGA onward (cluster LHH).

To get a more dynamic view of the functional incidence of transcriptome variations, we then analyzed transcripts overrepresented at each stage by grouping genes of several clusters according to prevalence of their transcripts at the four-cell, early morula, and blastocyst stage, respectively.

We performed an automated ontological analysis on transcripts present in the maternal inheritance at the four-cell stage (transcripts from clusters HLL, HHL, HLM, and MLH). At this stage, overrepresented molecular processes mainly involved amine, glycoprotein, and nitrogen compound metabolisms. "Aminoacyl tRNA ligase activity" remained intensively encoded by the maternal transcripts (Table 5). In contrast, biological processes concerning "transcription," "translation," "regulation of protein synthesis," and "chromosome or chromatin organization" were underrepresented, which was confirmed by the underrepresentation of molecular functions such as "structural constituent of ribosomes," "translation regulation activity," "translation factor activity," and "translation initiation factors" on the one hand and "transcription factor binding" on the other hand.

Interestingly, at EGA, analysis of transcripts from clusters HHL, LHL, and LHH revealed an overexpression of molecular processes involved in "RNA metabolism," including "mRNA and rRNA metabolism" and "RNA processing and splicing." Biological processes concerning macromolecule biosynthesis including "protein synthesis" were also overrepresented. Besides these activities, which were probably necessary to the modification in gene expression program occurring at that stage and which directly reflected the maternal to embryo transition in the control of development, we observed an overrepresentation of biological processes involved in "cell cycle" and "DNA integrity checkpoint." In contrast, biological processes linked to cell communication, such as "signal transduction" and "protein kinase cascades," were underrepresented.

When reaching the blastocyst stage (clusters LLH, HLM, LHH, MLH), the embryo transcriptome still encoded for "macromolecule and protein biosynthesis," but new synthesis activities appeared as overrepresented: these concerned "ATP metabolism" and "generation of precursor metabolites and energy"; also, "ion transport activities" appeared to be overrepresented in biological processes from this stage onward. Interestingly, "DNA and RNA metabolism," which were overrepresented at EGA, were underrepresented in the blastocyst transcriptome. In agreement with these results, the analysis of molecular functions at this stage pointed to a still high "structural constituent of ribosome" function, the appearance of "ion binding," "cation transporter," and "hydrolase and NADH dehydrogenase" activities, but also of a "peptidase" activity that was not represented until this stage and might be involved in the erasure of the maternally encoded program of gene expression.

We completed our functional analysis by comparing sets of genes according to the maternal or embryonic origin of their transcripts during the four-cell to blastocyst period of development. Therefore, the seven clusters of genes were regrouped in two sets. The first set gathered genes with maternal expression (*set 1* = clusters HLL + HHL + HLM + MLH), while the second set regrouped genes with an embryonic expression (*set 2* = clusters LLH + LHL + HLM + LHH + MLH). Both sets of genes were then pair-compared for their GO annotations. This analysis contrasted "transferase activities" including "kinase and phosphotransferase" molecular functions mainly encoded by maternal transcripts with "structural molecule," including "structural constituents of ribosome," "translation regulator," and "translation factor, nucleic acid binding" functions assumed by embryonic transcripts (Table 6).

In the rabbit species, transcriptional activation of the embryonic genome is very progressive and is only required to drive further development from the 8- to 16-cell stage onward. Both the total amount of RNA and the amount of messenger RNA are stable over the first cleavages (12, 23). Also, the protein content remains quantitatively stable until the morula stage (26), and the pattern of synthesis is only very progressively modified from the 2-cell to the 16-cell stage, with a large proportion of them still being translated from maternal transcripts (33). Both this apparent stability of the maternal legacy and the moderate epigenetic modifications of the embryonic genome at EGA (1, 31) raised the question of the control of gene expression over EGA and first differentiations in this species. To analyze this question, we focused on transcripts

Table 5. *Functional analysis of genes at each embryo stage*

GO	Name	GO Tree	All Array	Expressed at Stage	P Value	Over or Under
			Four-cell stage			
GO:0008150	Biological process	BP	582	210		
GO:0003674	Molecular function	MF	617	223		
GO:0006807	Nitrogen compound metabolism	BP	29	17	0.016	O
GO:0009308	Amine metabolism	BP	26	15	0.022	O
GO:0009101	Glycoprotein biosynthesis	BP	6	5	0.025	O
GO:0006325	Establishment and/or maintenance of chromatin architecture	BP	16	1	0.014	U
GO:0045449	Regulation of transcription	BP	96	24	0.014	U
GO:0051276	Chromosome organization and biogenesis	BP	24	3	0.015	U
GO:0042127	Regulation of cell proliferation	BP	10	0	0.016	U
GO:0006350	transcription	BP	101	26	0.017	U
GO:0004812	Aminoacyl-tRNA ligase activity	MF	10	8	0.006	O
GO:0004840	Ubiquitin-conjugating enzyme activity	MF	5	5	0.006	O
GO:0030955	Potassium ion binding	MF	6	5	0.025	O
GO:0003824	Catalytic activity	MF	274	112	0.035	O
GO:0045182	Translation regulator activity	MF	29	2	0.000	U
GO:0003735	Structural constituent of ribosome	MF	22	2	0.006	U
GO:0003676	Nucleic acid binding	MF	175	49	0.009	U
GO:0008134	Transcription factor binding	MF	18	2	0.025	U
GO:0003743	Translation initiation factor activity	MF	19	2	0.026	U
GO:0005198	Structural molecule activity	MF	34	6	0.026	U
			Early morula			
GO:0008150	Biological process	BP	582	163		
GO:0003674	Molecular function	MF	617	173		
GO:0016070	RNA metabolism	BP	78	36	0.000	O
GO:0006396	RNA processing	BP	66	32	0.000	O
GO:0042254	Ribosome biogenesis and assembly	BP	17	11	0.002	O
GO:0016072	rRNA metabolism	BP	11	8	0.002	O
GO:0006412	Protein biosynthesis	BP	72	31	0.003	O
GO:0000087	M phase of mitotic cell cycle	BP	14	9	0.005	O
GO:0044267	Cellular protein metabolism	BP	178	64	0.005	O
GO:0000398	Nuclear mRNA splicing, via spliceosome	BP	21	12	0.005	O
GO:0016071	mRNA metabolism	BP	44	21	0.005	O
GO:0006414	Translational elongation	BP	4	4	0.006	O
GO:0007028	Cytoplasm organization and biogenesis	BP	19	11	0.007	O
GO:0006397	mRNA processing	BP	42	20	0.007	O
GO:0019538	Protein metabolism	BP	195	67	0.019	O
GO:0031570	DNA integrity checkpoint	BP	3	3	0.022	O
GO:0006508	Proteolysis	BP	27	13	0.026	O
GO:0008380	RNA splicing	BP	41	18	0.029	O
GO:0007242	Intracellular signaling cascade	BP	33	2	0.002	U
GO:0007154	Cell communication	BP	68	10	0.009	U
GO:0048856	Anatomic structure development	BP	38	4	0.014	U
GO:0007165	Signal transduction	BP	64	10	0.018	U
GO:0051674	Localization of cell	BP	11	0	0.040	U
GO:0003723	RNA binding	MF	70	35	0.000	O
GO:0003735	Structural constituent of ribosome	MF	22	15	0.000	O
GO:0003676	Nucleic acid binding	MF	175	65	0.002	O
GO:0003746	Translation elongation factor activity	MF	3	3	0.022	O
GO:0015450	Protein translocase activity	MF	3	3	0.022	O
GO:0004888	Transmembrane receptor activity	MF	5	4	0.023	O
			Blastocyst			
GO:0008150	Biological process	BP	582	178		
GO:0003674	Molecular function	MF	617	190		
GO:0006119	Oxidative phosphorylation	BP	14	11	0.000	O
GO:0046034	ATP metabolism	BP	11	8	0.005	O
GO:0006508	Proteolysis	BP	27	15	0.009	O
GO:0006412	Protein biosynthesis	BP	72	31	0.020	O
GO:0006091	Generation of precursor metabolites and energy	BP	47	22	0.020	O
GO:0009059	Macromolecule biosynthesis	BP	75	32	0.022	O
GO:0044260	Cellular macromolecule metabolism	BP	180	67	0.025	O
GO:0006120	Mitochondrial electron transport, NADH to ubiquinone	BP	3	3	0.028	O
GO:0006397	mRNA processing	BP	42	6	0.015	U
GO:0006396	RNA processing	BP	66	12	0.023	U
GO:0016070	RNA metabolism	BP	78	15	0.024	U

Table 5.—*Continued*

GO	Name	GO Tree	All Array	Expressed at Stage	P Value	Over or Under
GO:0016071	mRNA metabolism	BP	44	7	0.027	U
GO:0006259	DNA metabolism	BP	48	8	0.033	U
GO:0008233	Peptidase activity	MF	22	14	0.001	O
GO:0015078	Hydrogen ion transporter activity	MF	16	11	0.002	O
GO:0003735	Structural constituent of ribosome	MF	22	13	0.008	O
GO:0008234	Cysteine-type peptidase activity	MF	6	5	0.012	O
GO:0015399	Primary active transporter activity	MF	17	10	0.016	O
GO:0005198	Structural molecule activity	MF	34	17	0.020	O
GO:0043169	Cation binding	MF	107	43	0.028	O
GO:0003746	Translation elongation factor activity	MF	3	3	0.029	O
GO:0008237	Metallopeptidase activity	MF	5	4	0.033	O
GO:0016758	Transferase activity, transferring hexosyl groups	MF	5	4	0.033	O
GO:0008324	Cation transporter activity	MF	26	13	0.048	O
GO:0000166	Nucleotide binding	MF	150	34	0.015	U
GO:0008415	Acyltransferase activity	MF	10	0	0.036	U

Data are GO categories from 2 branches of the GO tree (BP, MF) overrepresented (O) or underrepresented (U) among the genes expressed at each of the 3 embryo stages. Genes were considered expressed at the 4-cell stage if they belong to Hxx- or Mxx-type clusters, at the early morula if they belong to xHx-type clusters, and at the blastocyst stage if they belong to xxH- or xxM-type clusters. Lines without *P* value represent the total number of GO categories in a GO tree branch in the considered group of clusters.

expressed at EGA and at blastocyst stages by establishing a dedicated array.

The size of this first-generation array and the fact that only those maternal transcripts stable until the four-cell stage were represented make the functional transition between maternal legacy and early embryonic transcriptome difficult to compare with the data available in the mouse, where results are obtained on larger sets of genes (17, 34, 38), or even in the bovine (25) and the pig (35), where the stages analyzed are quite different from those involved in our study. However, our data point to the overrepresentation of genes involved in protein synthesis, RNA metabolism, and ribosome biogenesis and assembly among those genes transcribed at EGA, and this appears as a common trait in both mouse and rabbit models (38) despite their different EGA kinetics.

Our results also evidenced a highly dynamic transcriptome over the preimplantation period, and thus confirmed and extended some previous results established from the analyses of

Table 6. *Functional analysis of genes according to their maternal or embryonic status*

GO	Name	GO Tree	*Set 1* (maternal)	*Set 2* (embryonic)	P Value	Overrepresented
GO:0008150	Biological process	BP	210	224		
GO:0003674	Molecular function	MF	222	237		
GO:0006412	Translation	BP	16	33	0.007	E
GO:0022618	Protein-RNA complex assembly	BP	3	11	0.013	E
GO:0022613	Ribonucleoprotein complex biogenesis and assembly	BP	6	17	0.013	E
GO:0016043	Cellular component organization and biogenesis	BP	37	57	0.014	E
GO:0006417	Regulation of translation	BP	2	8	0.016	E
GO:0044249	Cellular biosynthetic process	BP	15	26	0.033	E
GO:0006414	Translational elongation	BP	0	4	0.044	E
GO:0006119	Oxidative phosphorylation	BP	7	14	0.048	E
GO:0006807	Nitrogen compound metabolic process	BP	17	7	0.007	M
GO:0006418	tRNA aminoacylation for protein translation	BP	8	2	0.011	M
GO:0009308	Amine metabolic process	BP	15	7	0.019	M
GO:0006519	Amino acid and derivative metabolic process	BP	14	7	0.032	M
GO:0006399	tRNA metabolic process	BP	8	3	0.045	M
GO:0007154	Cell communication	BP	33	24	0.047	M
GO:0005198	Structural molecule activity	MF	6	22	0.000	E
GO:0003735	Structural constituent of ribosome	MF	2	15	0.001	E
GO:0008135	Translation factor activity, nucleic acid binding	MF	2	13	0.005	E
GO:0045182	Translation regulator activity	MF	2	13	0.005	E
GO:0048037	Cofactor binding	MF	1	6	0.026	E
GO:0008237	Metallopeptidase activity	MF	1	6	0.026	E
GO:0008565	Protein transporter activity	MF	2	7	0.029	E
GO:0008233	Peptidase activity	MF	8	16	0.045	E
GO:0016740	Transferase activity	MF	33	18	0.005	M
GO:0004812	Aminoacyl-tRNA ligase activity	MF	8	2	0.012	M
GO:0016301	Kinase activity	MF	14	5	0.013	M
GO:0016773	Phosphotransferase activity, alcohol group as acceptor	MF	11	4	0.037	M

Data are GO categories from 2 branches of the GO tree (BP, MF) detected as overrepresented in the set of maternally expressed genes (M) or in the set of embryonically expressed genes (E). Genes were considered as maternally expressed if they belong to Hxx- or Mxx-type clusters and as embryonically expressed if they belong to xxH-, xxM-, or xHx-type clusters. Lines without *P* value represent the total number of GO categories in a GO tree branch.

only reduced numbers of candidate genes. First, the clustering pointed to at least three distinct kinetics of maternal transcript degradation between the four-cell stage and EGA: abrupt (clusters HLL and HLM), moderate (cluster MLH), or even apparently delayed (cluster HHL) degradation. Analysis of a few maternal transcripts over all the cleavage period had already evidenced differential regulation of maternal transcript stability in this species (18). Since our array displayed only a very partial population of maternal transcripts, we may hypothesize that the actual variability in maternal transcript regulation is even greater, especially between fertilization and four-cell stage. Second, regulation of embryonic transcript accumulation was also variable: their synthesis was either initiated at EGA (clusters LHL and LHH) or slightly delayed (clusters LLH, HLM, and MLH). Third, onset of embryonic transcript synthesis between EGA and blastocyst stage might be either progressive (clusters LLH, LHH, HLM, and MLH) or abrupt and transient (cluster LHL), confirming the data obtained by Pacheco-Trigon et al. (28) on a few candidate genes.

Interestingly, genes gathered in cluster LHL displayed the same regulative behavior as genes transiently expressed at the two-cell stage in the mouse embryo (17). Since the extent of epigenetic modifications of the embryonic genome that precede EGA is quite different in these species, we may hypothesize that transient expression of numerous genes at that stage did not result from an opportunistic mechanism due to the overall and abrupt demethylation of the genome but has a functional significance for ongoing development. Comparative analysis of the functions of these genes in both models is required to make this functional significance clearer. Although the analysis is still impaired by poor identification in the rabbit (57.6% unidentified genes in this cluster), the few functions evidenced by GO analysis of cluster LHL genes are quite different from those reported in the mouse (17). Additionally, several differences concerning the regulation of these genes may result from the differential kinetics of EGA between mouse and rabbit. In the mouse, genes transiently expressed at EGA displayed a second although weaker peak of transcription at the morula stage; in the rabbit, however, both of these peaks might gather into only one because of the delay in EGA. Also, a second cluster of transiently expressed genes was evidenced at the four-cell stage in the mouse embryo (17); our screening does not make it possible to identify such a cluster among the genes present in our array, but it may also be absent in the rabbit because of the kinetics of EGA. Whatever the case, however, functions identified in cluster LHL do not overlap those described for this second cluster in the mouse. Another difference between mouse and rabbit concerned the proportion of genes peaking at EGA in regard to long-term induced genes [LHL/(LLH + LHH)]: according to our data, this proportion is smaller in the rabbit than in the mouse embryo, which may also be related to the imminence of blastocyst formation that would require constant expression of some genes instead of transient and repeated peaks of expression. Moreover. in the rabbit, because of the delay in EGA, the decrease in expression of genes belonging to cluster LHL after EGA, which coincided with blastocyst formation, might be due either to an overall repression of transcription or to a restriction of expression to a specific cell lineage.

Conclusion. While no tool is available for the analysis of rabbit transcriptome, we established a first-generation array dedicated to early rabbit embryo and defined the conditions of its use to provide a dynamic view of embryo transcriptome during the period encompassing EGA and blastocyst formation. We demonstrated transient properties of gene expression pattern at EGA stage. This transient transcriptome is due not only to the concomitant decrease of maternal transcripts and accumulation of embryonic transcripts but also to the transient expression from the embryonic genome of a subset of genes the functions of which remain poorly characterized, but may be quite different from those observed in the mouse, for genes sharing a similar transient peak of expression at EGA. While further experiments are still necessary to better characterize these genes, the array is now being used to analyze perturbations of early embryo transcriptome according to alterations of embryo microenvironment.

REFERENCES

1. **Beaujean N, Hartshorne G, Cavilla J, Taylor J, Gardner J, Wilmut I, Meehan R, Young L.** Non-conservation of mammalian preimplantation methylation dynamics. *Curr Biol* 14: R266–R267, 2004.
2. **Beisvag V, Junge FK, Bergum H, Jolsum L, Lydersen S, Gunther CC, Ramampiaro H, Langaas M, Sandvik AK, Laegreid A.** GeneTools—application for functional annotation and statistical hypothesis testing. *BMC Bioinformatics* 7: 470, 2006.
3. **Bensaude O, Babinet C, Morange M, Jacob F.** Heat shock proteins, first major products of zygotic gene activity in mouse embryo. *Nature* 305: 331–333, 1983.
4. **Braude P, Bolton V, Moore S.** Human gene expression first occurs between the four- and eight-cell stages of preimplantation development. *Nature* 332: 459–461, 1988.
5. **Brinsko SP, Ball BA, Ignotz GG, Thomas PG, Currie WB, Ellington JE.** Initiation of transcription and nucleologenesis in equine embryos. *Mol Reprod Dev* 42: 298–302, 1995.
6. **Bui LC, Leandri RD, Renard JP, Duranthon V.** SSH adequacy to preimplantation mammalian development: scarce specific transcripts cloning despite irregular normalisation. *BMC Genomics* 6: 155, 2005.
7. **Camous S, Kopecny V, Flechon JE.** Autoradiographic detection of the earliest stage of [^{3}H]-uridine incorporation into the cow embryo. *Biol Cell* 58: 195–200, 1986.
8. **Christians E, Rao VH, Renard JP.** Sequential acquisition of transcriptional control during early embryonic development in the rabbit. *Dev Biol* 164: 160–172, 1994.
9. **Crosby IM, Gandolfi F, Moor RM.** Control of protein synthesis during early cleavage of sheep embryos. *J Reprod Fertil* 82: 769–775, 1988.
10. **Decraene C, Reguigne-Arnould I, Auffray C, Pietu G.** Reverse transcription in the presence of dideoxynucleotides to increase the sensitivity of expression monitoring with cDNA arrays. *Biotechniques* 27: 962–966, 1999.
11. **Didier G, Brezellec P, Remy E, Henaut A.** GeneANOVA—gene expression analysis of variance. *Bioinformatics* 18: 490–491, 2002.
12. **Duranthon V, Renard JP.** Storage and recovery of molecules in oocytes. In: *Biology and Pathology of the Oocyte*, edited by Trouson AO, Gosden RG. Cambridge: Cambridge Univ. Press, 2003, p. 81–112.
13. **Evsikov AV, de Vries WN, Peaston AE, Radford EE, Fancher KS, Chen FH, Blake JA, Bult CJ, Latham KE, Solter D, Knowles BB.**

Systems biology of the 2-cell mouse embryo. *Cytogenet Genome Res* 105: 240–250, 2004.

14. **Evsikov AV, Graber JH, Brockman JM, Hampl A, Holbrook AE, Singh P, Eppig JJ, Solter D, Knowles BB.** Cracking the egg: molecular dynamics and evolutionary aspects of the transition from the fully grown oocyte to embryo. *Genes Dev* 20: 2713–2727, 2006.

15. **Flach G, Johnson MH, Braude PR, Taylor RA, Bolton VN.** The transition from maternal to embryonic control in the 2-cell mouse embryo. *EMBO J* 1: 681–686, 1982.

16. **Fulka H, St John JC, Fulka J, Hozak P.** Chromatin in early mammalian embryos: achieving the pluripotent state. *Differentiation* 76: 3–14, 2008.

17. **Hamatani T, Carter MG, Sharov AA, Ko MS.** Dynamics of global gene expression changes during mouse preimplantation development. *Dev Cell* 6: 117–131, 2004.

18. **Henrion G, Brunet A, Renard JP, Duranthon V.** Identification of maternal transcripts that progressively disappear during the cleavage period of rabbit embryos. *Mol Reprod Dev* 47: 353–362, 1997.

19. **Johnson WH, Loskutoff NM, Plante Y, Betteridge KJ.** Production of four identical calves by the separation of blastomeres from an in vitro derived four-cell embryo. *Vet Rec* 137: 15–16, 1995.

20. **Ko MS, Kitchen JR, Wang X, Threat TA, Wang X, Hasegawa A, Sun T, Grahovac MJ, Kargul GJ, Lim MK, Cui Y, Sano Y, Tanaka T, Liang Y, Mason S, Paonessa PD, Sauls AD, DePalma GE, Sharara R, Rowe LB, Eppig J, Morrell C, Doi H.** Large-scale cDNA analysis reveals phased gene expression patterns during preimplantation mouse development. *Development* 127: 1737–1749, 2000.

21. **Latham KE.** Mechanisms and control of embryonic genome activation in mammalian embryos. *Int Rev Cytol* 193: 71–124, 1999.

22. **Latham KE, Solter D, Schultz RM.** Acquisition of a transcriptionally permissive state during the 1-cell stage of mouse embryogenesis. *Dev Biol* 149: 457–462, 1992.

23. **Manes C.** Nucleic acid synthesis in preimplantation rabbit embryos. I. Quantitative aspects, relationship to early morphogenesis and protein synthesis. *J Exp Zool* 172: 303–310, 1969.

24. **Manes C.** The participation of the embryonic genome during early cleavage in the rabbit. *Dev Biol* 32: 453–459, 1973.

25. **Misirlioglu M, Page GP, Sagirkaya H, Kaya A, Parrish JJ, First NL, Memili E.** Dynamics of global transcriptome in bovine matured oocytes and preimplantation embryos. *Proc Natl Acad Sci USA* 103: 18905–18910, 2006.

26. **Morgan PM, Kane MT.** Protein content of rabbit embryos: one cell to peri-implantation blastocyst. *J Reprod Fertil* 97: 101–106, 1993.

27. **Niwa H.** How is pluripotency determined and maintained? *Development* 134: 635–646, 2007.

28. **Pacheco-Trigon S, Hennequet-Antier C, Oudin JF, Piumi F, Renard JP, Duranthon V.** Molecular characterization of genomic activities at the onset of zygotic transcription in mammals. *Biol Reprod* 67: 1907–1918, 2002.

29. **Park JS, Jeong YS, Shin ST, Lee KK, Kang YK.** Dynamic DNA methylation reprogramming: active demethylation and immediate rem-ethylation in the male pronucleus of bovine zygotes. *Dev Dyn* 236: 2523–2533, 2007.

30. **Santos F, Hendrich B, Reik W, Dean W.** Dynamic reprogramming of DNA methylation in the early mouse embryo. *Dev Biol* 241: 172–182, 2002.

31. **Shi W, Dirim F, Wolf E, Zakhartchenko V, Haaf T.** Methylation reprogramming and chromosomal aneuploidy in in vivo fertilized and cloned rabbit preimplantation embryos. *Biol Reprod* 71: 340–347, 2004.

32. **Su YQ, Sugiura K, Woo Y, Wigglesworth K, Kamdar S, Affourtit J, Eppig JJ.** Selective degradation of transcripts during meiotic maturation of mouse oocytes. *Dev Biol* 302: 104–117, 2007.

33. **Tucker EB, Schultz GA.** Two-dimensional electrophoretic analysis of proteins synthesized during the early cleavage period in rabbit embryos. *Exp Cell Res* 114: 438–443, 1978.

34. **Wang QT, Piotrowska K, Ciemerych MA, Milenkovic L, Scott MP, Davis RW, Zernicka-Goetz M.** A genome-wide study of gene activity reveals developmental signaling pathways in the preimplantation mouse embryo. *Dev Cell* 6: 133–144, 2004.

35. **Whitworth KM, Agca C, Kim JG, Patel RV, Springer GK, Bivens NJ, Forrester LJ, Mathialagan N, Green JA, Prather RS.** Transcriptional profiling of pig embryogenesis by using a 15-K member unigene set specific for pig reproductive tissues and embryos. *Biol Reprod* 72: 1437–1451, 2005.

36. **Willadsen SM.** The viability of early cleavage stages containing half the normal number of blastomeres in the sheep. *J Reprod Fertil* 59: 357–362, 1980.

37. **Zeng F, Baldwin DA, Schultz RM.** Transcript profiling during preimplantation mouse development. *Dev Biol* 272: 483–496, 2004.

38. **Zeng F, Schultz RM.** RNA transcript profiling during zygotic gene activation in the preimplantation mouse embryo. *Dev Biol* 283: 40–57, 2005.